Adsorptive Sequestration of Cr(VI) using Chitosan-GBFS Composite

Apurva Bambal[1], Anita Shekhawat[1], Ravin Jugade[1*], Abbas Rahdar[2], Elvis Fosso-Kankeu[3], Sadanand Pandey[4,5*]

***Abstract*— :** Granulated blast furnace slag (GBFS)-chitosan crosslinked with epichlorohydrin was synthesized and applied for enhanced adsorption of hexavalent chromium from industrial effluent. The Chitosan-GBFS composite (Ch-GB) obtained was extensively characterized using instrumental techniques like FTIR, XRD, SEM-EDX etc. The composite showed adsorption capacity of 125.3 mg/g in accordance with Freundlich isotherm model at pH 3.0 due to presence of multiple sites which contribute for ion-pair and electrostatic interactions with Cr(VI) species. The sorption kinetics and thermodynamic studies revealed that adsorption of Cr(VI) followed by pseudo-second-order kinetics with exothermic and spontaneous behavior. The adsorbent was tested for regeneration for 5 adsorption-desorption cycles. The adsorbent could be regenerated and reused, which makes the study more environment friendly.

***Keywords*— :** Adsorption, chitosan, kinetics, Granulated blast furnace slag.

I. INTRODUCTION

Now-a-days, heavy metal pollution in environment is the biggest problem we are facing as a result of mainly mining activities [1-6]. Chromium is one of the heavy metals which cause acute or chronic diseases. Chromium is latent contaminant present in water as anthropogenic sources[7]. In nature, Chromium exists in two states[8], trivalent chromium and hexavalent chromium. For many organisms, trivalent chromium is essential element but hexavalent chromium is toxic as it intoxicates flora and fauna present in water bodies[9]. So, it is important to remove hexavalent chromium from water bodies.

There are various techniques such as coagulation, flocculation, ion exchange, membrane filtration, photo degradation, electrochemical process and microbial processes[10]. But to remove Cr(VI) from water bodies adsorption technique have been proven to be the best because of their effectiveness, low cost and selectivity. There are numerous biosorbents present in nature such as chitosan, cellulose, sodium alginate and starch[11] that possess the property of adsorption of Cr(VI). Chitosan was selected because it is second most available biosorbent in nature with another important property of biodegradability. Chitosan is linked by β-(1-4) glycosidic linkage[12].

Native chitosan has very less adsorption efficiency towards Cr(VI) ion. In order to improve this capacity, granulated blast furnace slag (GBFS) was trapped in the chitosan matrix using epichlorohydrin crosslinker. After composite formation the adsorption capacity was increased substantially.

II. MATERIALS AND METHOD

A. *Materials*

All the reagents used for adsorption of Chromium were of Analytical grade. Aqueous solutions were made by using double distilled water. Low molecular weight chitosan was procured from Sigma-Aldrich. Potassium dichromate, diphenyl carbazide was purchased from Loba Chemie Pvt. Ltd. Hydrochloric acid, Sulphuric acid and Epichlorohydrin were obtained from SD Fine Chemicals Pvt. Ltd. Granulated blast furnace slag (GBFS) was obtained from Tata steel plant, Bhilai, India.

B. *Preparation Of Ch-GB Composite*

3 g of Chitosan was dissolved in in 2% acetic acid solution. The solution was stirred for 60 min at room temperature. To it, 5 mL of epichlorohydrin was added to obtain pale yellow solution. The solution was further stirred for 30 min and 3 g of GBFS was added when a white color solution was obtained. Lastly, the resulting solution was precipitated into 3 M NaOH solution. The resulting Ch-GB composite was washed several times with double distilled water until the pH becomes neutral.

C. *Batch Adsorption Experiments*

To optimize pH, dose, contact time and chromium concentration, batch adsorption trails were studied by using 25 mL of Cr(VI) of desired concentration (10-500 mg/L) having pH (2-8) equilibrated with various Ch-GB doses (10-100 mg) for different time intervals (10-120 min) at desired

[1]Department of Chemistry, RTM Nagpur University, Nagpur-440033, India (ravinj2001@yahoo.co.in)

[2]Department of Physics, University of Zabol, Zabol, Iran.

[3]Department of Metallurgy, Faculty of Engineering and the Built Environment, Doornfontein Campus, University of Johannesburg, Johannesburg, South Africa

[4]School of Bioengineering and Food Technology, Faculty of Applied Sciences and Biotechnology, Shoolini University, Solan 173229, Himachal Pradesh, India (Sadanand.au@gmail.com)

[5]Department of Chemistry, College of Natural Science, Yeungnam University, 280 Daehak-Ro, Gyeongsan, Gyeongbuk, 38541, Republic of Korea

temperature. At equilibrium, concentration of Cr(VI) adsorbed on adsorbents was calculated as-

$$q_e = \frac{C_o - C_e}{W} \times V \quad (1)$$

Percentage adsorption capacity was also calculated by using equation (2) as follows.

$$\% \text{ Removal} = \frac{C_o - C_e}{C_o} \times 100 \quad (2)$$

C_0 and C_e are the initial and final equilibrium concentration of Cr(VI) solution in mg/L respectively. W is the weight of adsorbent in gram and V is the volume of Cr(VI) in L. Quantification of Cr(VI) was carried out spectrophotometrically using diphenyl carbazide reagent.

D. Instruments

The structural characterization of adsorbent Ch-GB composite was analyzed by using FTIR, XRD, and SEM-EDX. Bruker Alpha spectrometer was used to record FTIR spectra in range of 500-4000 cm^{-1}[13]. Righaku-Miniflex 300 x-ray diffractometer was used for XRD studies. The structural surface of composite was examined by using TESCAN VEGA 3 SBH. A Mac MSW-313 magnetic stirrer with temperature controller was employed for constant temperature study for thermodynamic parameter[12].

III. Results and Discussion

A. Ch-GB Characterization

The FT-IR spectral analysis of chitosan in Fig. 1 (a) showed distinct broad peaks corresponding to O-H and N-H stretching vibrations in region of 3898 and 3370 cm^{-1}, respectively. The peak at 2884 cm^{-1} was matched with -CH stretching peak. The spectrum also showed a peak at 1659 cm^{-1} indicating carbonyl of amide group. The peaks in region 1570 cm^{-1} and 1360 cm^{-1} was due to -NH and -H bending vibrations[14]. Additionally, Chitosan shows skeletal vibrations at 1003 cm^{-1} due to -C-O-C stretching[15]. Fig. 1 (b) depicts FT-IR spectra of GBFS which shows weak absorption peak at 3667 cm^{-1} and sharp absorption peak 997 cm^{-1} due to Si-Al-O stretching[16]. Fig. 1 (c) shows spectra for Ch-GB composite shows sharp peak at 561 cm^{-1} corresponding to symmetric stretching in siloxane group. The peaks due to -NH and -OH bending was obtained at 1583 cm^{-1} and 1355 cm^{-1}[17].

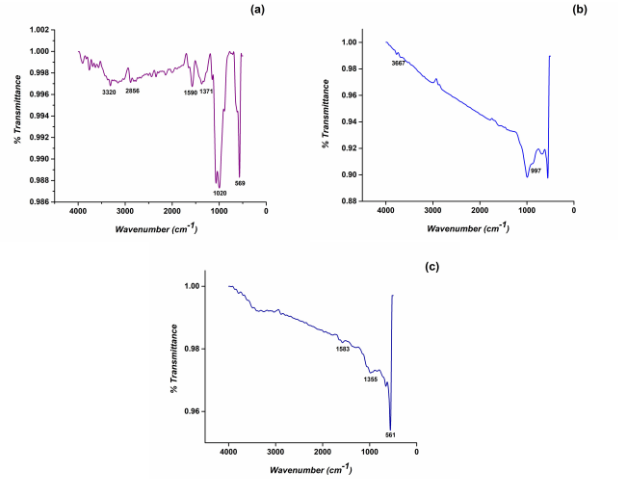

Fig. 1 FT-IR spectra (a) chitosan (b) GBFS (c) Ch-GB composite

The XRD spectra (Fig. 2) for pure chitosan has two characteristic peaks at 2θ values of 10.36^0 and 20.13^0[12]. The GBFS was found to be more crystalline with peaks at 31.08^0 and 44.65^0[18]. The Ch-GB composite shows all the peaks corresponding to chitosan as well as GBFS at 2θ values of 10.32^0, 20.15^0 and 44.54^0[19].

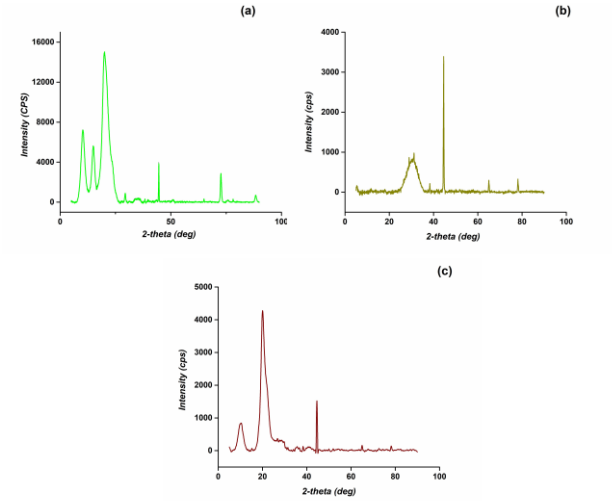

Fig. 2 XRD spectra of (a) chitosan (b) GBFS 9c) Ch-GB composite

The surface of native chitosan, pure GBFS and Ch-GB composite was inspected by SEM micrographs as shown in Fig. 3. Chitosan has irregular and loose surface morphology shown in Fig. 3 (a)[20]. While GBFS is having scaffold like morphology. SEM micrograph of Ch-GB adsorbent in Fig. 3 (c) is porous which is responsible for effective adsorption of Cr(VI)[21].

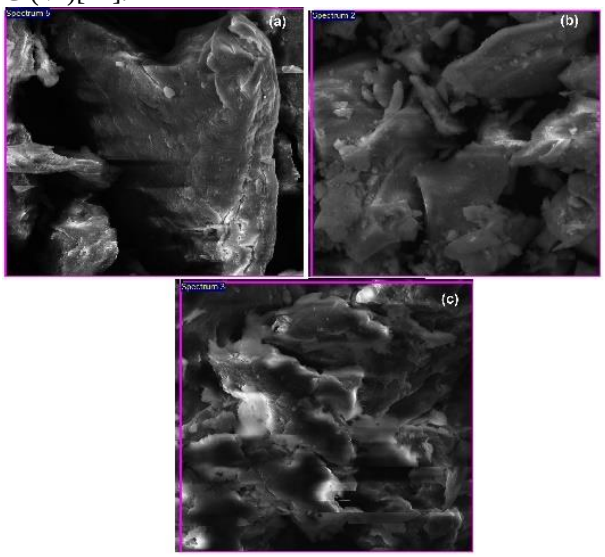

Fig. 3 SEM micrographs of (a) chitosan (b) GBFS (c) Ch-GB composite

EDX spectra of chitosan, GBFS and composite in Fig. 4 shows C,N and O peaks. EDX spectra of composite in Fig. 4 (c) show additional peaks of Si, Al and Mg[22].

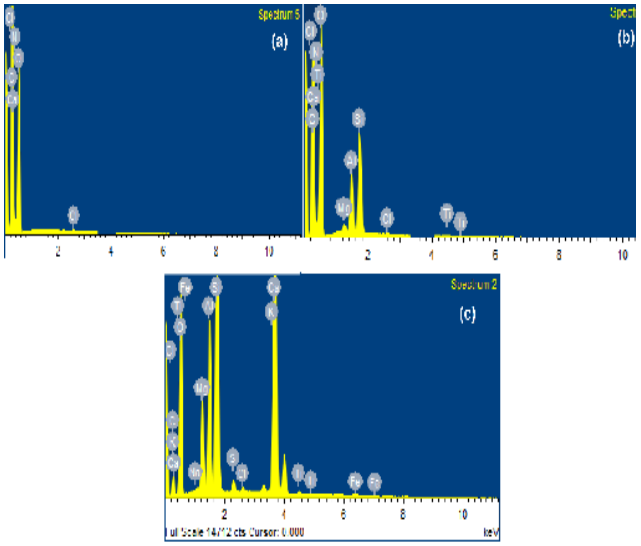

Fig. 4 EDX graph of (a) chitosan (b) GBFS (c) Ch-GB composite

B. Optimization of parameters

pH optimization is one of the vital parameters as it impacts surface charge of the adsorbent and also the species of adsorbent present in solution[23]. The effect of pH on adsorption of Cr(VI) was studied by using 100 mg L^{-1} concentration with 50 mg dose with varying pH from 3 to 8 and it was stirred for 60 min. Maximum adsorption of Cr(VI) was detected at pH 3. As pH increases, significant reduction in adsorption due to reduction in electrostatic interaction between adsorbate and adsorbent[24].

To optimize adsorbent dosage, dose was varied from 10 to 100 mg at 298 K at pH 3 for 60 min. As the dosage of adsorbent increased, the adsorption also increased reaching to a plateau after 50 mg dose. At 50 mg dose rate, the adsorbent showed maximum adsorption capacity. Hence 50 mg dose was selected for further studies.

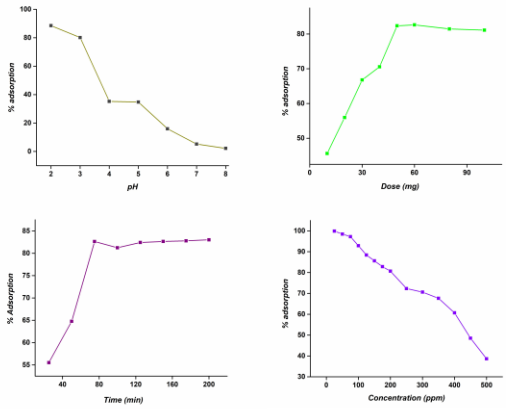

Fig. 5 (a) effect on pH (b) effect on dose (c) effect on time (d) effect on concentration

C. Adsorption isotherm studies

Langmuir and Freundlich adsorption isotherm models were used to study adsorption isotherms[25]. Fig. 5 depicts Langmuir and Freundlich model which correlates experimental values obtained by varying concentration of adsorbate solution[26].

The Ch-GB composite exhibits maximum adsorption capacity (q_m) of 125.32 mg/g for Cr(VI). The value of R^2 was found out to be 0.982 for Freundlich adsorption isotherm. The value of R^2 was close to unity, hence Freundlich model was best fitted model. Non-linear plots for both isotherms were showed in Fig. 6. Supplementary information was listed in Table I.

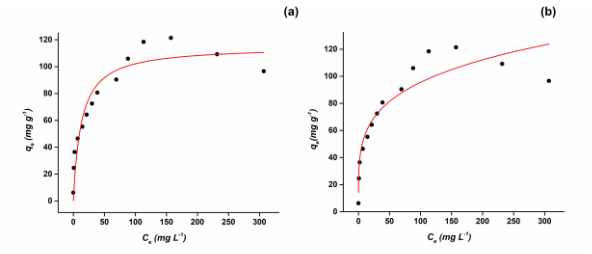

Fig. 6 Adsorption isotherm model (a) Langmuir (b) Freundlich

TABLE I
ISOTHERM PARAMETERS

Isotherm	Parameters	Cr(VI)
Langmuir	q_m (mg/g)	125.32
	R_L	0.98
	R^2	0.904
Freundlich	K_f ($mg^{1-1/n}/g/L$)	10.62
	n	1.627
	R^2	0.998

D. Adsorption Kinetics

The influence of contact time on adsorption capacity was studies by using kinetic parameter[27]. Two models were assessed for kinetic study. Pseudo first order as well as pseudo second order model were used[28]. Non- linear fitment plots were showed in Fig. 7. Contact time was varied from 10 to 120 min.

From the calculations and graph, it was found that pseudo-second-order model was best suited for this study because the value of R^2 was found out to be 0.997. Values for kinetic study are listed in Table II.

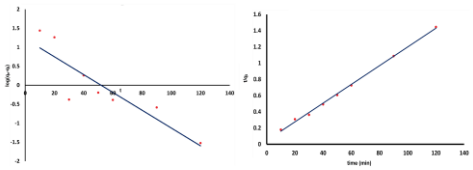

Fig. 7 (a) Pseudo first order kinetics (b) Pseudo second order kinetics

TABLE II
KINETIC PARAMETERS

Isotherm	Parameter	Cr(VI)
Pseudo-first-order	K_1	0.054
	R^2	0.782
Pseudo-second-order	K_2	5.188
	R^2	0.998
Intraparticle diffusion	$i_{intercept}$	67.03
	R^2	0.420

E. Adsorption Thermodynamics

Effect of temperature on adsorption efficiency was studied by varying temperature from 298 to 323 K by keeping rest parameters constant[29]. Gibbs free energy change was assessed by using thermodynamic equilibrium constant i.e. K. As the value of ΔG is negative over entire temperature range, hence the reaction becomes spontaneous[29]. The negative value of ΔH calculated from Van't Hoffs plot indicates exothermic nature of reaction while negative value for ΔS indicated that the adsorbate is going from solution to solid phase. Hence from above discussion, the process is enthalpy driven in nature. The values for adsorption thermodynamics and Van't Hoff plot were shown in Fig. 8.

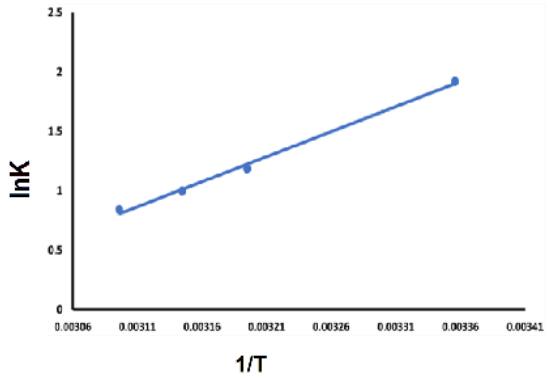

Fig. 8 Van't Hoff graph plotted 1/T versus lnK

TABLE III
THERMODYNAMIC PARAMETERS

Temperature (K)	ΔG (kJ/mol)	ΔS (J/mol/K)	ΔH (kJ/mol)
298	-2.064	-44.24	-15.23
313	-1.338		
318	-1.143		
323	-0.981		

F. Regeneration of adsorbate

To study regeneration factor of adsorbate, many reagents were used NaCl, NaOH, Na_2SO_4 and Na_2CO_3. Amongst all, desorption pattern for Ch-GB composite was studied with 5% NaOH. To study the effectiveness of adsorbate, seven adsorption-desorption cycles were performed which was shown in Fig. 9[30]. Adsorption efficiency was more than 80% after first cycle, depicting that the composite can be regenerated and reused.

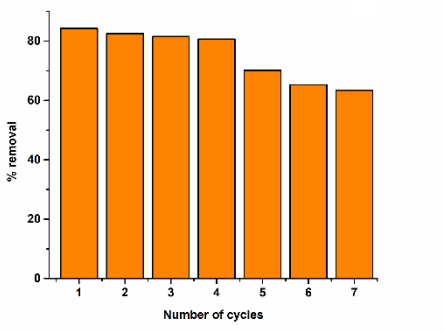

Fig. 9 Efficiency of regenerated material

IV. CONCLUSION

Native Chitosan has low adsorption capacity towards adsorption of Cr(VI) ions. To increase the effectiveness of adsorption it was crosslinked with epichlorohydrin and GBFS resulting into composite Ch-GB which shows maximum adsorption capacity of 125.32 mg/g at pH 3, dose 50mg, contact time 60 min and concentration 200 mg/L at 298 K following Freundlich adsorption isotherm. Fitting of kinetics model having R^2 value close to unity confirms pseudo-second-order. In general, GBFS is waste of steel industry and it can be used to increase effectiveness of adsorption of Cr(VI). Also, the composite formed was reused and regenerated which make it more ecofriendly.

REFERENCES

[1] S. Gupta and S. Pilani, "Adsorption of Chromium (VI) by a Low-Cost Adsorbent Prepared from Tamarind Seeds," no. May, 2014, [Online]. Available: http://discovery.bits-pilani.ac.in/~bvbabu/AD_SG_BVB_Chemcon-2006_FullPaper.pdf

[2] E. Fosso-Kankeu, A. Mulaba-Bafubiandi, B.B. Mamba, T.G. Barnard. Assessing the effectiveness of a biological recovery of nickel from tailings dumps. Journal of Minerals Engineering.Vol 24, pp 470-472, 2011.

[3] E. Fosso-Kankeu, F.B. Waanders, F.W. Steyn. The Preparation and Characterization of Clay-Biochar Composites for the Removal of Metal Pollutants. 7th International Conference on Latest Trends in Engineering and Technology (ICLTET' 2015), November 26-27, 2015 Irene, Pretoria (South Africa). Editors: E. Muzenda and T Yingthawornsuk. ISBN: 978-93-84422-58-5, 2015.

[4] E. Fosso-Kankeu, F. Waanders, E. Maloy. Copolymerization of ethyl acrylate onto guar gum for the adsorption of Mg(II) and Ca(II) ions. Desalination and Water Treatment. doi: 10.1080/19443994.2016.1165147: 1-10, 2016.

[5] L.C. Razanamahandry, C.T. Onwordi, W. Saban, A.K.H. Bashir, L. Mekuto, E. Malenga, E. Manikandan, E. Fosso-Kankeu, M. Maaza, S.K.O. Ntwampe. Performance of various cyanide degrading bacteria on the biodegradation of free cyanide in water. Journal of Hazardous Materials. 380: 1-6, 2019.

[6] V. S. Wadi, H. Mittal, E. Fosso-Kankeu, K.K. Jena, S.M. Alhassan. Mercury removal by porous sulphur copolymers: Adsorption isotherm and kinetics studies. Colloids and Surfaces A. 606: 125333-125343, 2020.

[7] M. Nur-E-Alam, M. Abu Sayid Mia, F. Ahmad, and M. Mafizur Rahman, "Adsorption of chromium (Cr) from tannery wastewater using low-cost spent tea leaves adsorbent," *Appl. Water Sci.*, vol. 8, no. 5, pp. 1–7, 2018, doi: 10.1007/s13201-018-0774-y.

[8] P. E. Dim, L. S. Mustapha, M. Termtanun, and J. O. Okafor, "Adsorption of chromium (VI) and iron (III) ions onto acid-modified kaolinite: Isotherm, kinetics and thermodynamics studies," *Arab. J. Chem.*, vol. 14, no. 4, p. 103064, 2021, doi: 10.1016/j.arabjc.2021.103064.

[9] S. Mor, K. Ravindra, and N. R. Bishnoi, "Adsorption of chromium from aqueous solution by activated alumina and activated charcoal," *Bioresour. Technol.*, vol. 98, no. 4, pp. 954–957, 2007, doi: 10.1016/j.biortech.2006.03.018.

[10] A. Baran, E. Biçak, Ş. H. Baysal, and S. Önal, "Fabrication of Next-Generation Multifunctional LBG-s-AgNPs@ g-C3N4 NS hybrid nanostructures for Environmental Applications," *Envirnmental Research.*, 117540, 2024, doi:10.1016/j.envres.2023.117540.

[11] D. Mohan and C. U. Pittman, "Activated carbons and low cost adsorbents for remediation of tri- and hexavalent chromium from water," *J. Hazard. Mater.*, vol. 137, no. 2, pp. 762–811, 2006, doi: 10.1016/j.jhazmat.2006.06.060.

[12] A. Ayub, Z. A. Raza, M. I. Majeed, M. R. Tariq, and A. Irfan, "Development of sustainable magnetic chitosan biosorbent beads for kinetic remediation of arsenic contaminated water," *Int. J. Biol. Macromol.*, vol. 163, pp. 603–617, 2020, doi: 10.1016/j.ijbiomac.2020.06.287.

[13] S. Korde, S. Tandekar, C. Jeyaseelan, D. Saravanan, and R. Jugade, "Mesoporous magnetic Chitosan-Zirconia-Iron oxide nanocomposite for adsorptive removal of Cr(VI) ions," *Mater. Lett.*, vol. 311, no. December 2021, 2022, doi: 10.1016/j.matlet.2021.131513.

[14] A. Pawlak and M. Mucha, “Thermogravimetric and FTIR studies of chitosan blends,” *Thermochim. Acta*, vol. 396, no. 1–2, pp. 153–166, 2003, doi: 10.1016/S0040-6031(02)00523-3.

[15] E. M. Eddarai, M. El Mouzahim, R. Boussen, A. Bellaouchou, A. Guenbour, and A. Zarrouk, “Chitosan-kaolinite clay composite as durable coating material for slow release NPK fertilizer,” *Int. J. Biol. Macromol.*, vol. 195, no. December 2021, pp. 424–432, 2022, doi: 10.1016/j.ijbiomac.2021.12.055.

[16] D. A. Metlenkin *et al.*, “Identification of the Elemental Composition of Granulated Blast Furnace Slag by FTIR-Spectroscopy and Chemometrics,” *Processes*, vol. 10, no. 11, 2022, doi: 10.3390/pr10112166.

[17] M. Zhu *et al.*, “Strengthening mechanism of granulated blast-furnace slag on the uniaxial compressive strength of modified magnesium slag-based cemented backfilling material,” *Process Saf. Environ. Prot.*, vol. 174, no. April, pp. 722–733, 2023, doi: 10.1016/j.psep.2023.04.031.

[18] J. Zhao *et al.*, “Hydration superposition effect and mechanism of steel slag powder and granulated blast furnace slag powder,” *Constr. Build. Mater.*, vol. 366, no. December 2022, p. 130101, 2023, doi: 10.1016/j.conbuildmat.2022.130101.

[19] X. Han *et al.*, “Preparation, characterization and antibacterial activity of new ionized chitosan,” *Carbohydr. Polym.*, vol. 290, no. March, p. 119490, 2022, doi: 10.1016/j.carbpol.2022.119490.

[20] M. M. Armendáriz-Ontiveros *et al.*, “Modification of Thin Film Composite Membrane by Chitosan–Silver Particles to Improve Desalination and Anti-Biofouling Performance,” *Membranes (Basel).*, vol. 12, no. 9, 2022, doi: 10.3390/membranes12090851.

[21] L. Yan *et al.*, “Efficient removal of Cr(VI) by the modified biochar with chitosan schiff base and MnFe2O4 nanoparticles: Adsorption and mechanism analysis,” *J. Environ. Chem. Eng.*, vol. 11, no. 2, p. 109432, 2023, doi: 10.1016/j.jece.2023.109432.

[22] R. El Kaim Billah *et al.*, “Adsorptive removal of Cr(VI) by Chitosan-SiO2-TiO2 nanocomposite,” *Environ. Nanotechnology, Monit. Manag.*, vol. 18, no. April, 2022, doi: 10.1016/j.enmm.2022.100695.

[23] Z. Huang *et al.*, “Facile synthesis of a MOF-derived magnetic CoAl-LDH@chitosan composite for Pb (II) and Cr (VI) adsorption,” *Chem. Eng. J.*, vol. 449, no. April, p. 137722, 2022, doi: 10.1016/j.cej.2022.137722.

[24] S. H. Vithalkar and R. M. Jugade, “Adsorptive removal of crystal violet from aqueous solution by cross-linked chitosan coated bentonite,” *Mater. Today Proc.*, vol. 29, pp. 1025–1032, 2020, doi: 10.1016/j.matpr.2020.04.705.

[25] L. Natrayan, V. Swamy Nadh, K. M. Katubi, D. Ali, and D. G. Lemu, “Adsorption of SO2on ZnO Nanowires Using Activated Carbon by Langmuir Adsorption Isotherm,” *Adsorpt. Sci. Technol.*, vol. 2022, 2022, doi: 10.1155/2022/1287890.

[26] M. Musah, Y. Azeh, J. Mathew, M. Umar, Z. Abdulhamid, and A. Muhammad, “Adsorption Kinetics and Isotherm Models: A Review,” *Caliphate J. Sci. Technol.*, vol. 4, no. 1, pp. 20–26, 2022, doi: 10.4314/cajost.v4i1.3.

[27] Q. Hu, S. Pang, and D. Wang, “In-depth Insights into Mathematical Characteristics, Selection Criteria and Common Mistakes of Adsorption Kinetic Models: A Critical Review,” *Sep. Purif. Rev.*, vol. 51, no. 3, pp. 281–299, 2022, doi: 10.1080/15422119.2021.1922444.

[28] V. Gomase, R. Jugade, P. Doondani, D. Saravanan, and S. Pandey, “Sequential modifications of chitosan biopolymer for enhanced confiscation of Cr(VI),” *Inorg. Chem. Commun.*, vol. 145, no. September, p. 110009, 2022, doi: 10.1016/j.inoche.2022.110009.

[29] A. Shekhawat, S. Kahu, D. Saravanan, S. Pandey, and R. Jugade, “Rational modification of chitosan biopolymer for remediation of Cr(VI) from water,” *J. Hazard. Mater. Adv.*, vol. 7, no. July, p. 100123, 2022, doi: 10.1016/j.hazadv.2022.100123.

[30] R. M. Jugade, “and Phosphate Ions,” no. Iii, 2022.